

Numerical study of thermal runaway caused by local overheating of LiFePO₄ battery

Xu Luo¹, Xueqiang Li¹, Yabo Wang¹, Shengchun Liu¹, Hailong Li^{1,2*}

¹ Tianjin Key Laboratory of Refrigeration Technology, Tianjin University of Commerce, Tianjin 300134, China

² School of Sustainable Development of Society and Technology, University of Mälardalen, Västerås 72123, Sweden

ABSTRACT

Thermal runaway of battery leads to a serious consequence, such as explosion, in which the variation of temperature is the key parameter needed to be controlled. Therefore, by using the validated 3D model, this paper discussed the impact of discharge rate and convection heat transfer coefficient on the behavior of thermal runaway, which is caused by the local overheating. Results showed that, a high discharge rate could increase the rate of temperature rise and decrease the triggering time of thermal runaway. It changed from 895 s to 771 s when the discharge rate increased from 0.5 C to 4 C. Increasing the convection heat transfer coefficient was an effective way to mitigate the thermal runaway. Compared to 15 W/(m²·K), the highest temperature of battery could decrease by 40 °C and the triggering time could be delayed by 280 s when the convection heat transfer coefficient was 75 W/(m²·K). The result obtained in this paper could provide guidance to understand the characteristic of thermal runaway.

Keywords: lithium-ion battery, thermal runaway, local overheating, safety

NONMENCLATURE

Abbreviations

SEI	Solid electrolyte layer
MSMD	Multi-scale multi-domain
DOD	Depth of discharge

1. INTRODUCTION

With the development of electric vehicles (EVs) and hybrid electric vehicles (HEVs), the demand of battery with low cost and high performance becomes urgent. Lithium-ion battery is the optimal choice due to the high energy density and high operating voltage [1, 2]. However, the application is limited by the operating temperature of the battery [3-5]. If beyond the optimal range (25 - 40 °C), the performance would be decreased.

Moreover, extreme condition, such as thermal runaway should be also considered, which is usually caused by mechanical abuse, electrical abuse, and thermal abuse [6, 7]. Overheating is a typical scenario in thermal abuse, leading to a lot of heat [10], resulting in the high temperature of battery and generation of gas smoke, fire, and explosion.

There have some literatures focusing on the thermal runaway. Feng et al. [11] explored the characteristic of thermal runaway for large-size prismatic battery by the extended volume-accelerating rate calorimetry. By using three important temperatures, i.e., abnormal heat starting temperature, triggering temperature, and maximum temperature, the process of thermal runaway could be better described. Lopez et al. [12] tested the behavior of thermal runaway for 18650 lithium battery. Results showed maximum temperature rise increased with the increase of temperature in the ambient if the heat power was constant. Lei et al. [10] found the temperature rise increased with the increase of heating temperature. And the heating area showed slight impact on it. Zhang et al. [13] found though the heat produced by internal short circuit was a small part for the total heat, it was still a key factor inducing the thermal runaway.

Therefore, due to the complex process of thermal runaway, this paper established a coupled model, including the thermal model, the electrochemical model, and thermal runaway model, to explore the characteristic of thermal runaway. By using the validated model, the effect of discharge rate and convection heat transfer coefficient on thermal runaway are carefully discussed, during which the triggering time, the rate of temperature rise, and the maximum temperature were employed as the performance indicators. The results obtained in this paper could provide guidance to understand the characteristics of thermal runaway.

2. MODEL DESCRIPTION AND VALIDATION

2.1 Model description

Fig. 1 shows the battery model studied in this paper. It consists of battery and heater. The dimension of battery is 175 mm × 205 mm × 30 mm, with 86 Ah of capacity. The end of discharge and discharge voltages are 2 V and 3.65 V, respectively. The thickness of heater is 30 mm and its length and width are same with that of battery. During operation, 500 W of heating power is conducted on the heater to heat the battery and induce the thermal runaway. The thermal runaway can be divided into three stages: (1) the pre-thermal runaway development, which consists of the SEI film decomposition reaction; (2) the rapid thermal run-away development stage, which consists of the redox reaction between the cathode, anode and electrolyte; (3) the end of thermal runaway, where the internal reaction gradually stops and the temperature decreases slowly.

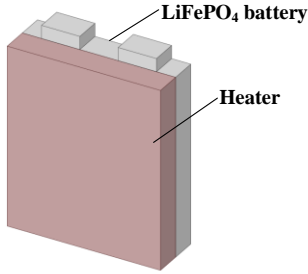


Fig. 1 Battery and heater construction

To establish the 3D model, the thermal model, the electrochemical model, and thermal runaway model are needed. For thermal model, the continuity equation, the momentum equation, and the energy equation can be found in the following:

$$\frac{\partial \rho_1}{\partial t} + \text{div}(\rho_1 U) = 0 \quad (1)$$

$$\begin{cases} \frac{\partial(\rho_1 u)}{\partial t} + \text{div}(\rho_1 u U) = \text{div}(\mu \text{grad} u) - \frac{\partial p}{\partial x} + S_u \\ \frac{\partial(\rho_1 v)}{\partial t} + \text{div}(\rho_1 v U) = \text{div}(\mu \text{grad} v) - \frac{\partial p}{\partial y} + S_v \\ \frac{\partial(\rho_1 w)}{\partial t} + \text{div}(\rho_1 w U) = \text{div}(\mu \text{grad} w) - \frac{\partial p}{\partial z} + S_w \end{cases} \quad (2)$$

$$\rho_2 C_p \frac{dT}{dt} = -\nabla \cdot (k \nabla T) + S \quad (3)$$

where, ρ_1 is the air density; U is the velocity vector. u , v , and w are the velocity components of the velocity vector in the x , y , and z directions, respectively. μ is the aerodynamic viscosity; S_u , S_v , S_w are the generalized source terms of the momentum conservation equation. ρ_2 is the density of the cell component, C_p is the specific the heat capacity, T is the cell temperature, k is the thermal conductivity of the cell, and S is the source term i.e., the heat generation rate per unit volume, which

consists of the chemical exothermic reaction of the component and the internal short circuit.

For electrochemical model, multi-scale multi-domain (MSMD) is selected [14]. It can be described as:

$$j_{ECh} = \frac{Q_{nominal}}{Q_{ref} Vol} Y [U - Y] \quad (4)$$

$$\begin{cases} Y = \left(\sum_{n=0}^5 b_n (DoD)^n \right) \exp \left[-C_1 \left(\frac{1}{T} - \frac{1}{T_{ref}} \right) \right] \\ U = \left(\sum_{n=0}^5 a_n (DoD)^n \right) - C_2 (T - T_{ref}) \end{cases} \quad (5)$$

$$DoD = \frac{Vol}{3600 Q_{nominal}} \int_0^t j dt \quad (6)$$

where, Vol represents the single cell active area volume, V is the single cell volt-age, $Q_{nominal}$ represents total battery power and Q_{ref} represents the battery capacity, which is used in the experiments to obtain the model parameters Y and U , where Y and U are functions of the battery depth of discharge (DOD). C_1 and C_2 are specific constants. the Y and U parameters are extracted from the battery dis-charge at different multipliers tests.

For thermal runaway model, it can be found in the following:

$$\begin{cases} \frac{dc_{sei}}{dt} = -A_{sei} \exp \left[-\frac{E_{sei}}{RT} \right] c_{sei}^{m_{sei}} \\ \frac{dc_{ne}}{dt} = -A_{ne} \exp \left[-\frac{t_{sei}}{t_{sei,ref}} \right] \exp \left[-\frac{E_{ne}}{RT} \right] c_{ne}^{m_{ne}} \\ \frac{d\alpha}{dt} = A_{pe} \exp \left[-\frac{E_{pe}}{RT} \right] \alpha^{m_{pe,1}} (1-\alpha)^{m_{pe,2}} \\ \frac{dc_e}{dt} = -A_e \exp \left[-\frac{E_e}{RT} \right] c_e^{m_e} \end{cases} \quad (7)$$

where, A , E and m are reaction kinetic parameters, denoting the exponential prefactors, activation energy, and reaction order, respectively; the subscripts sei , ne , pe , and e denote the parameters associated with the SEI layer decomposition reaction, negative electrode reaction with electrolyte, positive electrode reaction with electrolyte, and electrolyte decomposition reaction, respectively; C_{sei} , C_{ne} , C_e , and α are dimensionless variables; t_{sei} is a dimensionless measure of the SEI layer thickness; $t_{sei,ref}$ is the reference SEI layer thickness; T is the ambient temperature; R is the gas constant.

2.2 Key performance indicator

In order to better understand the characteristic of thermal runaway, triggering time, the rate of temperature rise, and maximum temperature are employed as the performance indicator. For triggering time, it can be obtained through the following:

$$t_{ir} = t_{T_2} \quad (8)$$

where, t_{T_2} is the time to reach the T2, and T2 is the critical point between gradual and sharp increase in temperature, i.e., the trigger temperature for thermal runaway.

For maximum temperature, it can be described as:

$$T_{\max} = T_3 \quad (9)$$

where, T_3 is the maximum temperature during thermal runaway.

For the rate of temperature rise, it can be found in the following:

$$\Delta T = \frac{T_3 - T_2}{t_{T_{\max}} - t_{T_2}} \quad (10)$$

where, $t_{T_{\max}}$ is the time to reach the maximum temperature.

2.3 Grid independence test and Model Validation

Table 1 shows the grid independence test. It can be found when the grid number was larger than 164138, triggering time and maximum temperature did not vary. Therefore, 164138 was selected to do the following work.

Table. 1 Grid independence test

Grid number	Triggering time/s	Maximum temperature/°C
81740	884	352
164138	883	353
277200	883	353

To validate the proposed model, reference [13] was employed. In this work, the heater is located on the side of the battery and acts as a heat source to trigger the thermal runaway of the battery. Insulating cotton covers both sides of the battery and heater to reduce heat dissipation to the environment and fixture tools. Based on this, Fig. 2 shows the result of model validation. It was clear that the simulation result was agreement with experimental data for both heating process and thermal runaway process. The maximum temperature difference was 14 °C occurred at 817 s, which was mainly caused by the valve opening causing the battery to drop in temperature over a short period of time. Therefore, the model was considered as validated and can be used to predict the characteristic of thermal runaway.

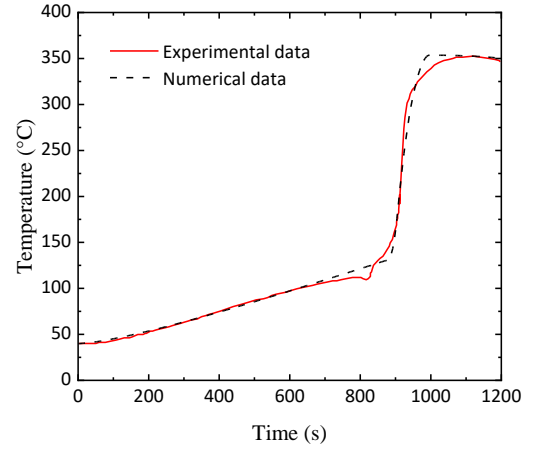
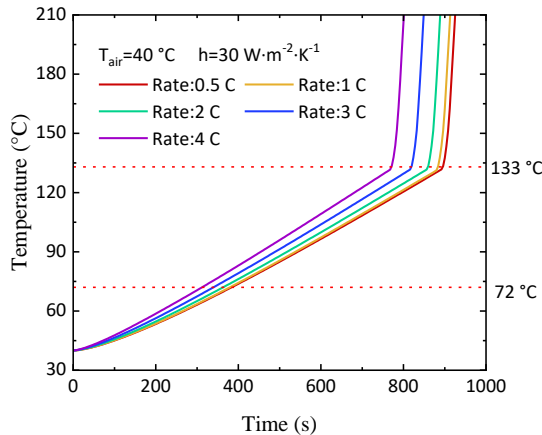


Fig. 2 Model validation

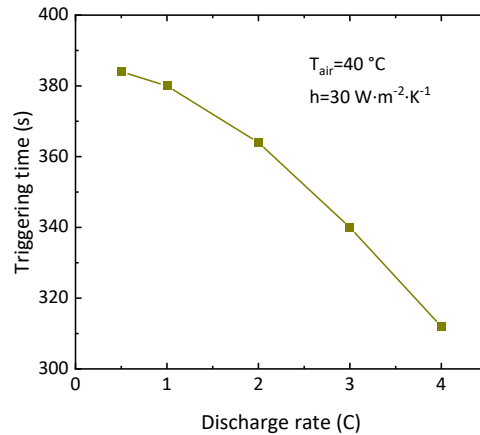
3. RESULTS AND ANALYSIS

3.1 Effect of discharge rate on thermal runaway

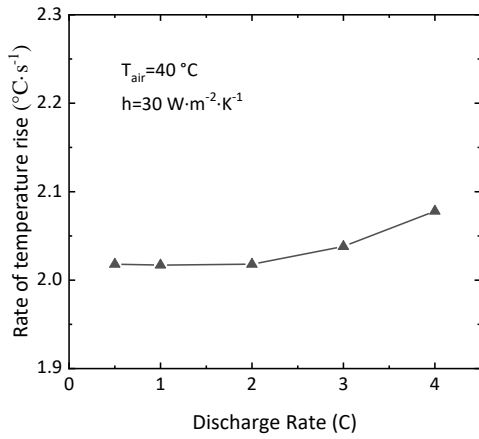
Fig. 3 shows the impact of discharge rate on the characteristic of thermal runaway. In the heating process, the temperature linearly increased with the time. High discharge rate would also increase the temperature at the same time, as shown in Fig. 3(a). Therefore, triggering time of thermal runaway would be advanced, as shown in Fig. 3(b). Compared to 0.5 C of discharge rate, it would be increased by 12 s, 36 s, 76 s and 124 s for 1 C, 2 C, 3 C, and 4 C, respectively. In the meantime, the rate of temperature rise was also different under different discharge rate. Since the start of heating to battery failure, high discharge rate would also increase the rate of temperature rise, as shown in Fig. 3(c). It should be note that, the maximum temperature of battery was not changed with the variation of discharge rate. This was mainly due to the fact that the maximum temperature of thermal runaway is influenced by the thermal properties of the battery material, independent of the discharge rate, as shown in Fig. 3 (d).



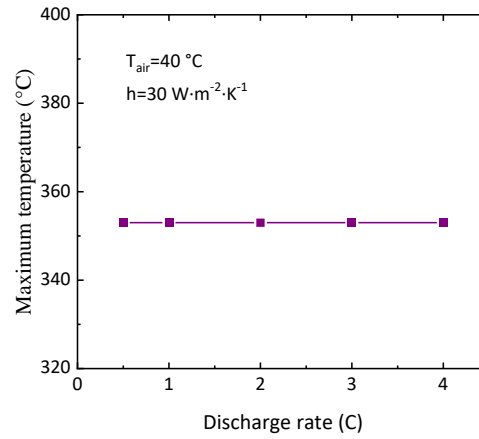
(a) Temperature variation of before and after thermal runaway



(b) Effect of discharge rate on the triggering time



(c) Effect of discharge rate on the rate of temperature rise



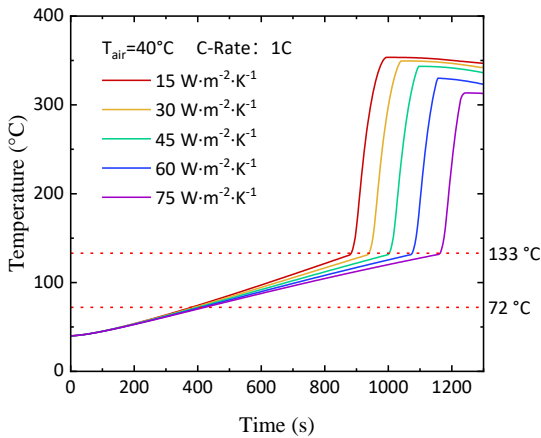
(d) Effect of discharge rate on the maximum temperature

Fig. 3 Effect of discharge rate on thermal runaway

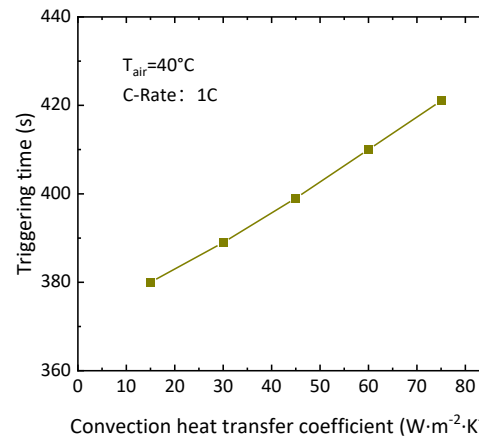
3.2 Effect of convective heat transfer coefficient on thermal runaway

Fig. 4 shows the impact of convection heat transfer coefficient on the characteristic of thermal runaway. Large convection heat transfer coefficient was benefit to the heat dissipation of battery. Similarly with the impact of discharge rate, the temperature linearly increased during the heating process. And high convection heat transfer coefficient could delay the happen of thermal runaway, as shown in Fig. 4(a) and Fig. 4(b). For example,

the triggering time were 883 s, 1003 s, 1075 s, and 1163 s for 15 W/(m²·K), 30 W/(m²·K), 45 W/(m²·K), 60 W/(m²·K), and 75 W/(m²·K), respectively. In addition, since more heat can be dissipated at large convection heat transfer coefficient, the rate of temperature rise and maximum temperature would also decrease. For example, the rate of temperature rise and maximum temperature were 0.19 °C/s and 353 °C at 15 W/(m²·K); while these values were 0.17 °C/s and 313 °C at 75 W/(m²·K).



(a) Temperature variation of before and after thermal runaway



(b) Effect of convection heat transfer coefficient on the triggering time

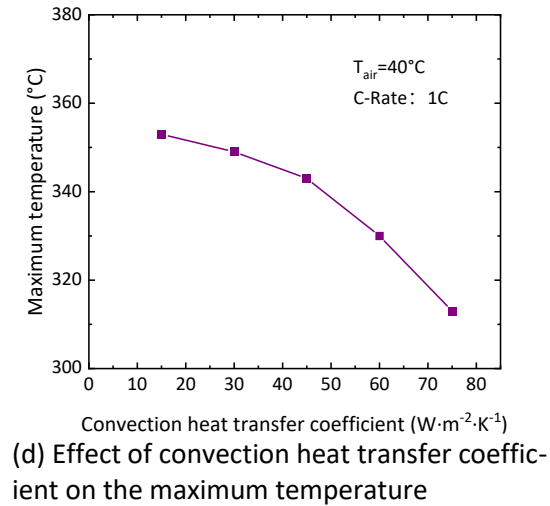
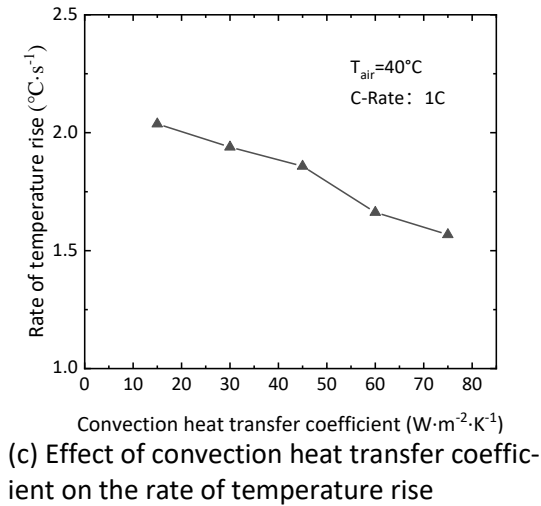


Fig. 4 Effect of convective heat transfer coefficient on thermal runaway

4. CONCLUSIONS

The coupled model, including thermal model, the electrochemical model, and thermal runaway model, was established and validated in this paper to explore the characteristic of thermal runaway of battery. The impact of discharge rate and convection heat transfer coefficient on thermal runaway was carefully discussed. Through the result, it can be concluded that:

(1) High discharge rate would deteriorate the thermal runaway, including the triggering time and the rate of temperature rise. However, the maximum temperature was slightly affected by the discharge rate.

(2) Since large convection heat transfer coefficient could dissipate more heat timely, it could alleviate the thermal runaway, including the triggering time, rate of temperature rise, and the maximum temperature of battery.

ACKNOWLEDGEMENT

This work was funded by Science and Technology Program of Tianjin, China (No. 2021ZD031).

REFERENCE

[1] Schaltz E, Stroe D et al: Incremental capacity analysis applied on electric vehicles for battery state-of-health estimation. *IEEE Transactions on Industry Applications*. 2021;57(2):1810-1817.
 [2] Adaikkappan M, Sathiyamoorthy N. Modeling, state of charge estimation, and charging of lithium-ion battery in electric vehicle: a review. *International Journal of Energy Research*.2022; 46(3): 2141-2165.
 [3] Kong D, Wang G, Ping P et al. Numerical investigation of thermal runaway behavior of lithium-ion batteries with different battery materials and heating conditions. *Applied Thermal Engineering*.2021;189:116661.

[4] Zhou Z, Zhou X, Cao B et al. Investigating the relationship between heating temperature and thermal runaway of prismatic lithium-ion battery with LiFePO₄ as cathode. *Energy*.2022;256:124714.
 [5] Panchal S, Dincer I, Agelin-Chaab M et al. Thermal modeling and validation of temperature distributions in a prismatic lithium-ion battery at different discharge rates and varying boundary conditions. *Applied Thermal Engineering*.2016;96:190-199.
 [6] Duh Y S, Sun Y, Lin X et al. Characterization on thermal runaway of commercial 18650 lithium-ion batteries used in electric vehicles: A review. *Journal of Energy Storage*. 2021;41:102888.
 [7] Lai X, Yi W, Cui Y et al. Capacity estimation of lithium-ion cells by combining model-based and data-driven methods based on a sequential extended Kalman filter. *Energy*.2021;216:119233.
 [8] Wang J, Mei W, Cui Z et al. Experimental and numerical study on penetration-induced internal short-circuit of lithium-ion cell. *Applied Thermal Engineering*.2020;171:115082.
 [9] Ren D, Feng X, Lu L et al. Overcharge behaviors and failure mechanism of lithium-ion batteries under different test conditions. *Applied Energy*.2019;250:323-332.
 [10] Lei Z, Maotao Z, Xiaoming X et al. Thermal runaway characteristics on NCM lithium-ion batteries triggered by local heating under different heat dissipation conditions. *Applied Thermal Engineering*.2019;159:113847.
 [11] Feng X, Zheng S, Ren D, et al. Investigating the thermal runaway mechanisms of lithium-ion batteries based on thermal analysis database. *Applied energy*. 2019, 246: 53-64.
 [12] Lopez C F, Jeevarajan J A, Mukherjee, P P. Characterization of lithium-ion battery thermal abuse behavior using experimental and computational analysis. *Journal of The Electrochemical Society*.2015;162(10): A2163.

- [13] Zhang Y, Mei W, Qin P et al. Numerical modeling on thermal runaway triggered by local overheating for lithium iron phosphate battery. *Applied Thermal Engineering*.2021;192:116928.
- [14] Kwon K H, Shin C B, Kang T H et al. A two-dimensional modeling of a lithium-polymer battery. *Journal of Power Sources*.2006;163(1):151-157.
- [15] Kim G H, Pesaran A, Spotnitz, R. A three-dimensional thermal abuse model for lithium-ion cells. *Journal of power sources*.2007;170(2):476-489.
- [16] Hatchard T D, MacNeil D D, Basu A et al. Thermal model of cylindrical and prismatic lithium-ion cells. *Journal of The Electrochemical Society*.2001;148(7):A755.